Energy Conversion and Management 315 (2024) 118739

Contents lists available at ScienceDirect

Energy Conversion and Management

journal homepage: www.elsevier.com/locate/enconman

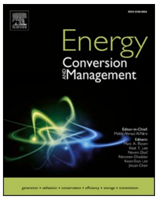

Solid oxide fuel cells with integrated direct air carbon capture: A techno-economic study

Imogen Griffiths, Ruiqi Wang [*], Janie Ling-Chin, Anthony Paul Roskilly

Department of Engineering, Durham University, Durham DH1 3LE, UK

ARTICLE INFO

Keywords:
Direct air carbon capture
Solid oxide fuel cells
Hydrogen
Levelised cost

ABSTRACT

Direct air carbon capture, as a negative emissions technology, is pivotal to lowering carbon dioxide concentration in the atmosphere. Accompanying the development and application of this technology, the high energy demand and substantial capital cost associated with direct air carbon capture have been persistent concerns. This paper aims to analyse the technical and economic feasibility of utilising a hydrogen fed solid oxide fuel cell as a source of both electricity and high-grade heat for the process of direct air carbon capture. It is vital that a renewable form of hydrogen production is used for this process to be sustainable, therefore a renewable hydrogen fed 50 MW solid oxide fuel cell is modelled, integrated with a direct air carbon capture process, resulting in a system with the capacity to remove carbon dioxide just over 270 kt/year directly from the air. The current levelised cost of capture for the system varies widely with the price of renewable hydrogen production, with an estimated range of £314–1,505 per tonne of carbon dioxide captured. As the cost of renewable hydrogen declines in the future, such a process could become a feasible alternative to natural gas fed direct air capture, with a 2050 levelised cost of capture anticipated to be £191 per tonne.

1. Introduction

The ongoing reliance on the combustion of fossil fuels to provide energy has driven a critical increase in atmospheric carbon dioxide (CO_2) concentration, rising from ~ 280 ppm to 419 ppm over the last century and a half [1]. With the ratification of the Paris Agreement in 2015, international governments share a common objective to limit the global average temperature increase to 1.5 °C above pre-industrial levels. As a primary greenhouse gas (GHG), the importance of reducing CO_2 emissions to manage its atmospheric concentration cannot be overstated. Negative emissions technology (NET) has become an area of increasing interest for academics, industry, and policymakers, with one of the most promising solutions being the direct capture of CO_2 from ambient air (DAC) [1]. Benefitting from relatively low land and water requirements, and an inherent flexibility of placement, DAC could systematically manage presently unavoidable emissions such as those from the aviation sector and heavy industry, and has potential to remove up to 12 Gt CO_2 per year [2,3].

Based on the mechanisms of capture and separation/regeneration, DAC has been classified into five categories: liquid scrubbing, solid sorbent, electrochemical, membrane, and cryogenic [4]. The two most plausible DAC technologies are solid sorbent DAC (S-DAC) and liquid solvent-based DAC (L-DAC). S-DAC employs solid sorbents to adsorb CO_2 from the air, which can be regenerated under temperature/pressure/vacuum-swing conditions [5]. The main advantages of S-DAC reflect on the low capital cost and low-temperature regeneration. But it is important to note that many current solid sorbents have relatively low CO_2 selectivity and could adsorb water at the same time [2]. The S-DAC also faces the challenge of operation in batches, as it needs periodically to be isolated from the ambient air during sorbents' regeneration [6]. In contrast, L-DAC has advantage on the higher absorption capacity and the benefit of continuous operation, which promotes it suitable for large scale DAC operations (0.5–1 Mt/year) [4]. The L-DAC was proposed by Lackner et al [7] when DAC was initially introduced in the late 1990 s. Compared to flue gas carbon capture technologies, L-DAC captures CO_2 from ambient air in which concentration of CO_2 is 350 times lower than CO_2 concentration in flue gas [8]. To capture 1 Mt/year of CO_2, air with 400 ppm CO_2 needs to be pumped through a contactor of L-DAC at a rate of 46,000 m^3/s [9]. With an air velocity of 1.5 m/s, a contactor surface area of 38,000 m^2 is required to achieve a capture rate of 75 % [10]. The regeneration process of L-DAC is energy-intensive, requiring high-temperature heat at around 900 °C [11]. Commercial firm Carbon Engineering (CE) has piloted L-DAC process with electricity demand of 366

---

[*] Corresponding author.
E-mail address: ruiqi.wang@durham.ac.uk (R. Wang).

https://doi.org/10.1016/j.enconman.2024.118739
Received 2 August 2023; Received in revised form 21 June 2024; Accepted 25 June 2024
Available online 1 July 2024

Nomenclature

AC_{HX}	Area of heat exchanger, m^2
AC_{SOFC}	Area of solid oxide fuel cell stack, m^2
C_{fuel}	Price of hydrogen, £/kg
$C_{fuel,t}$	Price of hydrogen in year *t*, £/kg
C_{HX}	Cost of heat exchanger, £
C_{SOFC}	Cost of solid oxide fuel cell stack, £
$C_{SOFC,aux}$	Cost of solid oxide fuel cell auxiliaries, £
$C_{SOFC,DC/AC}$	Cost of DC-AC inverter, £
$C_{SOFC,rep}$	Replacement cost of solid oxide fuel cell, £
$CapEx_{DAC}$	Total capital cost of direct air capture, £/tCO_2
$CapEx_{SOFC}$	Total capital cost of solid oxide fuel cell, £
$\dot{E}_{calciner}$	Energy supplied to the calciner, MW_{th}
F	Faraday constant, 96,485 A•s/mol
i	Internal rate of return
I_{SOFC}	Current generated by solid oxide fuel cell, A
I_C	Current density, mA/cm^2
I_t	Investment cost in year t, £
h	Specific enthalpy of flow, MW
h_{cath}	Specific enthalpy of cathode exhaust, MW
h_{steam}	Specific enthalpy of steam, MW
k	Capacity factor
$LCOA$	Levelised cost of capture from air, £/tCO_2
$LCOE$	Levelised cost of electricity, £/$MW_{el}h$
LHV_{fuel}	Lower heating value of fuel, MJ/kg
LR	Annual debt, £
$\dot{m}$	Mass flow rate, kg/s
$\dot{m}_{cath}$	Mass flow rate of cathode exhaust, kg/s
$\dot{m}_{CO2}$	Mass flow rate of CO_2, kg/s
$\dot{m}_{excess}$	Mass flow rate of unburnt fuel from the anode exhaust gas, kg/s
$\dot{m}_{fuel}$	Mass flow rate of fuel supplied to solid oxide fuel cell, kg/s
$\dot{m}_{steam}$	Mass flow rate of steam from anode, kg/s
M_{DAC}	Plant capture capacity, tCO_2/year
n	Project's lifetime, year
n_{H_2}	Mole flow rate of reacted H_2, mol/s
$n_{O_2,consumed}$	Mole flow rate of consumed O_2 at cathode, mol/s
$n_{O_2,in}$	Mole flow rate of input O_2 to cathode, mol/s
$OpEx_{DAC}$	Total operating cost of direct air capture, £/tCO_2
$OpEx_{SOFC,fixed}$	Fixed operating cost of solid oxide fuel cell, £
$OpEx_{SOFC,var}$	Variable operating cost of solid oxide fuel cell, £
P_{H2}	Partial pressure of hydrogen, bar
P_{H2O}	Partial pressure of steam, bar
P_{O2}	Partial pressure of oxygen, bar
P_{ref}	Reference pressure of solid oxide fuel cell, bar
P_{SOFC}	Operating pressure of solid oxide fuel cell, bar
$\dot{q}_{calciner}$	Specific energy consumption of the calciner, MJ/kg
$\dot{Q}_{calciner}$	Thermal energy supplied to the calciner, MW_{th}
t	Year *t*
T_{SOFC}	Operating temperature of solid oxide fuel cell, °C
T_{ref}	Reference temperature of solid oxide fuel cell, °C
U_a	The air utilisation of the solid oxide fuel cell
U_f	The fuel utilisation of the solid oxide fuel cell
V_{ref}	Reference voltage, mV
V_{SOFC}	Actual voltage of solid oxide fuel cell, V
$\dot{W}_{cal}$	Specific power consumption of calciner, kWh/tCO_2
$\dot{W}_{com}$	Specific power consumption of CO_2 compressor, kWh/tCO_2
$\dot{W}_{fan}$	Specific power consumption of air contactor fan, kWh/tCO_2
$\dot{W}_{net}$	Net power output of the system, MW_{el}
$\dot{W}_p$	Parasitic load of direct air capture process, MW_{el}
$\dot{W}_{pump}$	Specific power consumption of fluid pump, kWh/tCO_2
$\dot{W}_{sla}$	Specific power consumption of slaker, kWh/tCO_2
$\dot{W}_{SOFC}$	Power generated by solid oxide fuel cell, MW_{el}
$\dot{W}_{SOFC,DC}$	Rated/direct current power output of solid oxide fuel cell, kW_{el}
z	The number of electrons transferred per reaction
ΔV_{anode}	Correction of reference voltage due to variation in the fuel composition, mV
$\Delta V_{cathode}$	Correction of reference voltage due to variation in the oxidant composition, mV
ΔV_T	Correction of reference voltage due to variation in the actual temperature and current density, mV
ΔV_p	Correction of reference voltage due to variation in the actual pressure, mV
$\eta_{AC/DC}$	AC-DC conversion efficiency
η_{net}	Net system efficiency
η_{SOFC}	Thermal efficiency of solid oxide fuel cell

Abbreviations

CC	Carbon capture
CE	Carbon Engineering
CHP	Combined heat and power
DAC	Direct air carbon capture
DC	Direct current
KPI	Key performance indicator
GHG	Greenhouse gas
L-DAC	Liquid solvent-based direct air carbon capture
LCOA	Levelised cost of capture from air
LCOE	Levelised cost of electricity
NET	Negative emissions technology
Ni-YSZ	Nickel-yttria stabilised zirconia
PPA	Power purchase agreement
S-DAC	Solid sorbent-based direct air carbon capture
SOFC	Solid oxide fuel cell

kWh/tCO_2 and heat demand of 5.3 GJ/tCO_2 [6]. But these amounts of requisite energy were met entirely by natural gas, which would cause extra on-site CO_2 emissions and diminish the carbon reduction efficiency of L-DAC. Therefore powering DAC with renewable energy is a more sustainable avenue [12]. Innovation to support renewable energy options for high-temperature industrial heat has been recognised as an effective method to maximise the carbon removal potential of L-DAC plants [3].

Numerous studies have been made by researchers regarding supplying energy to DAC through low-carbon or renewable energy sources. For instance, the DAC was assessed in combination with excess solar and wind energy to capture 500 Mt of CO_2 in Europe [13], and 140 Mt of CO_2 in the US [1]. With a mix of low-carbon electricity and heat supplied through solar collectors, a net carbon removal of high-temperature L-DAC has been evaluated up to 73 % per tonne of CO_2 captured and stored [14]. By using solar energy coming from a heliostat field, the heat from solar energy can reach up to 1,000 °C and was investigated to drive the calcination process [15]. However, the efficiency of the solar-driven calcination process is highly dependent on the receiver performance, and renewable energy sources always exhibit intermittent properties [16], which may render the continuous operation of DAC incompatible with renewable energy. Additionally, the size and land use of renewable energy installations will be significant for their integration with L-DAC. For example, to capture 1 Mt of CO_2 per year, it was determined that a solar field with 1,420 MW and an area of 2.47 km^2 would be needed at a location with high solar irradiation [17]. Similarly, capturing the same amount CO_2 per year would require 240 MW wind power and a wind farm with an area of 54 km^2 [18]. In this way, waste heat source was considered as an alternative heat source due to its low cost and less burden in environmental impact, verifying its linkage with DAC [3]. Waste heat can potentially be sourced from combined heat and power plants [19]. But studies have indicated that coupling DAC with waste heat from power generation streams would be more favourable for the solid sorbent DAC which requires much lower quality of heat ranging 70 °C–100 °C [20]. Although high-grade waste heat around 900 °C can be acquired from cement kiln, ceramics industry or metal processing plants, etc., it is always fed back into the existing system [21]. To achieve simultaneous supply of high-grade waste heat and renewable electricity to DAC, solid oxide fuel cell (SOFC) was considered to be integrated with DAC [22]. SOFCs are high temperature fuel cells, which convert the chemical energy of fuel directly into electricity and heat when an additional oxidant is provided. Their high temperature operation within the stack yields notable residual heat to calcine a carbonate material [8]. Importantly, SOFCs have outstanding fuel flexibility, with the most common options being fuelled by natural gas, biomass and hydrogen [23].

SOFC has been integrated with carbon capture (CC) technologies [24]. For instance, Rao et al. [25] presented a novel SOFC combined heat and power (CHP) system fed by coke oven gas from steel industry, where CO_2 from anode off-gas is captured by pressure swing adsorption, resulting in a reduction of 50 % in CO_2 emissions for equal power production. In a biomass gasification combined SOFC system, exhaust gases from SOFC was decarbonised by absorption solution, thereby allowing for net CO_2 emissions from power generation of SOFC [26]. Santarelli et al. [27] examined the role of SOFC in performing carbon recovery and re-utilisation, by placing an oxy-fuel combustor downstream the SOFC to alter cathode off-gas composition from H_2 and CO to H_2O and CO_2, after which CO_2 was captured and supplied to a photobioreactor. Although these studies combined CC technologies with SOFC, the role of CC was mainly to mitigate resulting inherent CO_2 emissions from SOFC's off-gas due to combustion of carbon-based fuel gas at the anode of SOFC. Therefore, these CC technologies focused more on the commonly available post-combustion capture and oxy-fuel combustion capture which are suitable for gases with higher CO_2 concentration. For a DAC system linked to a SOFC, the main objective of CC technology is to remove CO_2 from the air, while the SOFC is used to provide the power and heat needed for the DAC process. Hanak et al. [8] processed a combined SOFC and L-DAC plant where the waste exhaust gases of a natural gas fed SOFC were used to provide electricity and high-grade heat for the calcination process without offering CaO regeneration and calcined products. A kW scale SOFC was demonstrated to integrate with a calciner, where high-grade heat from the anode off-gas was used to drive the calcination process [28]. Such a system provided technical feasibility of using SOFC as power and heat sources to calcination process. Erans et al. [29] tested different steam-rich conditions simulating flue gas from a SOFC on the calcination process, and subsequent DAC performance of the calcined materials, showing significant effect of steam on the duration of calcination and suitability of the calcines for DAC. Thus, current research on the DAC-SOFC has primarily investigated on the calcination process, and rarely investigated whole process of DAC from air contactor to CO_2 compressor. Similarly, the SOFCs in these studies are fed by the fuel gas that emits CO_2. To avoid additional CO_2 emissions from anode gases of the integrated DAC-SOFC system, hydrogen shows promising potential as the fuel gas. When hydrogen is

Table 1
Previous techno-economic study of integrated DAC system.

Ref.	Scope	Processes modelled	Analysis method	Key findings
Hanak et al. [8]	Utilisation of high-grade heat from a SOFC to drive the calcination process in a once-through DAC concept	Calcination process of DAC, natural gas fed SOFC	Techno-economic analysis and parametric studies	The process has the potential to remove 463.5–882.3 g $CO_2/kW_{el}h$ and achieves LCOE of £50/$MW_{el}h$
Hanak and Manovic [30]	Polygeneration for CHP using a SOFC and lime production for DAC	Calcination process, heat exchanger network, natural gas fed SOFC, fresh material	Thermodynamic and economic analysis	Due to high capital requirement of the SOFC, the capital cost is estimated as £744.6/kW_{ch}
Daniel et al. [31]	DAC process integrated with a solid oxide electrolysis for the chemical utilisation of the captured CO_2	L-DAC process (hydrogen as fuel for calciner), solid oxide electrolysis cell	Economic analysis	The LCOA shows a high value initially, at \$382/tCO_2, but could be reduced with the advances of technology maturity and the net zero economy
An et al. [32]	Assessment of the impact of climate conditions on L-DAC, CO_2 capture rate, and cost of DAC	Natural gas standalone and grid-electricity connected L-DAC system	Thermodynamic and economic analysis	The LCOA of natural gas standalone scenario varies from \$240/tCO_2 to \$409/tCO_2, and is more sensitive to temperature
Moreno-Gonzalez et al. [33]	Production of syngas by using CO_2 sourced from solvent based DAC	Air contactor and natural gas fed calcium loop process, syngas synthesis, CO_2 electrolysis	Levelised cost of syngas and energy efficiency analysis	Levelised cost of syngas is around 1 \$/kg. Energy-efficient and cost-competitive DAC-carbonate-electrolysis needs cheaper electricity and membrane
Prats-Salvado et al. [34]	Integration of DAC with concentrated solar power and further methanol synthesis	L-DAC (powered by grid, solar, and oxyfuel mixture), solid sorbent DAC (powered by grid and waste heat), thermochemical cycle, methanol synthesis process	Economic analysis including net present value and cash flow	The most economical methanol is produced with a central solid sorbent DAC that consumes the low-quality waste heat from the downstream process
Coppitters et al. [35]	Methanation utilising CO_2 captured from power grid by solid sorbent DAC with waste heat recovery	Solid sorbent DAC (fuelled by waste heat from electrolyser), electrolyser, methanation unit	Energy, exergy, economic, and environmental analysis	The exergy efficiency is mainly due to the uncertainty of the ambient conditions, and the levelised cost of synthetic natural gas ranges between 130 €/MWh and 744 €/MWh
Datta and Krishnamoorti [36]	Integration of DAC with wind energy and with proximal use in enhanced oil recovery	Adsorption-based DAC (powered by wind energy), membrane-based DAC, enhanced oil recovery	Levelised cost of DAC, cumulative cost, and profitability analysis	Lower LCOE of \$25/MWh yielded a cost of DAC of \$3–\$7/tCO_2
Sabatino et al. [37]	DAC process combining KOH scrubbing with bipolar membrane electrodialysis	Air contactor, bipolar-anion exchange membrane, bipolar-cation exchange membrane	Multi-objective optimisation, economic and energy evaluation	Energy cost can be reduced by improving cell conductivity. The levelized cost of the air capture units is \$49–77/tCO_2
J. Sagues [38]	Biomass energy integrated with DAC system	Natural gas fed-L-DAC, biomass gasification fed-L-DAC, biomass boiler fed-solid sorbent carbon capture and DAC	Levelised cost of CO_2 removal, capital cost expenditure, net operating cost	Levelised costs of CO_2 removal by the biomass fed L-DAC and natural gas fed L-DAC range from \$54–187/tCO_2 and \$65–268/tCO_2, respectively

produced from electrolysis, whereby electrolysis is powered by renewable energy, there is potential to maximise the efficiency of a hydrogen fed SOFC integrated DAC system in carbon reduction to create a truly sustainable NET.

Table 1 summarises a literature review on previous analysis of integrated DAC system. The review showed that the technical and economic feasibility of the proposed integrated renewable hydrogen fed SOFC and L-DAC system has not been investigated before. As both L-DAC and SOFCs are commercially immature, pricing estimates vary widely, which presents the need for exploring the parameters and process settings of the system. Thus, this study is novel as it fills this research gap by developing a detailed model of the integrated DAC-SOFC fed by renewable hydrogen. Appropriate economic assumptions to estimate key techno-economic parameters for the whole process are also established in this study, including the levelised cost of capture from air (LCOA) and levelised cost of electricity (LCOE) to determine its viability, both with current prices and prices in a possible 2050 scenario.

2. Materials and methods

To analyse the techno-economic viability of L-DAC, a model was created in AspenPlus v12.2 to represent the process, the behaviour of the SOFC and the integration of the L-DAC and the SOFC systems. Key parameters were chosen to assess the performance of the proposed system. A model validation was performed against CE's L-DAC system [6] and an natural gas fed SOFC system [39]. From a thermodynamic perspective, the optimal setup for the process was identified and the impact of changing thermodynamic parameters on performance was assessed. An economic analysis was included, exploring the sensitivity of the system's levelised costs when significant parameters such as hydrogen fuel prices are altered. To account for future pricing changes, a 2050 economic scenario was modelled including predictions of key parameters such as SOFC unit prices and the price of hydrogen fuel. As such, the techno-economic viability of such a system both in the present and in the future was assessed.

3. Model description

In AspenPlus v12.2, the L-DAC model was modelled based on CE's industrial scale process designed by Keith et al. [6], which applied conventional natural gas combustion for energy generation, for which an AspenPlus model was created by Bianchi et al. [40]. The SOFC system was modelled based on the natural gas fed SOFC model reported by Hanak et al. [8] to provide heat and electricity to a once-through DAC process. The SOFC unit itself was adjusted based on the Zhang et al.'s [39] natural gas fed model to accommodate pure hydrogen as a fuel. The integrated hydrogen fed DAC-SOFC system consisted of six key components: the air contactor, the pellet reactor, the steam slaker, the calciner, the CO_2 compression unit, and the SOFC, as shown in Fig. 1. Details of each component and the reactions involved were described in the following subsections. Temperatures, mass flow rates and enthalpies of each stream, mass and energy balances, as well as the characteristics of each AspenPlus component used to create the model in every block were provided in **Supplementary Information (S.1– S.9)**.

3.1. Direct air carbon capture

The L-DAC process was suggested by Keith et al. [6] and highlighted here: during the process, ambient air is drawn through the air contactor unit, where its CO_2 content reacts with the aqueous potassium hydroxide

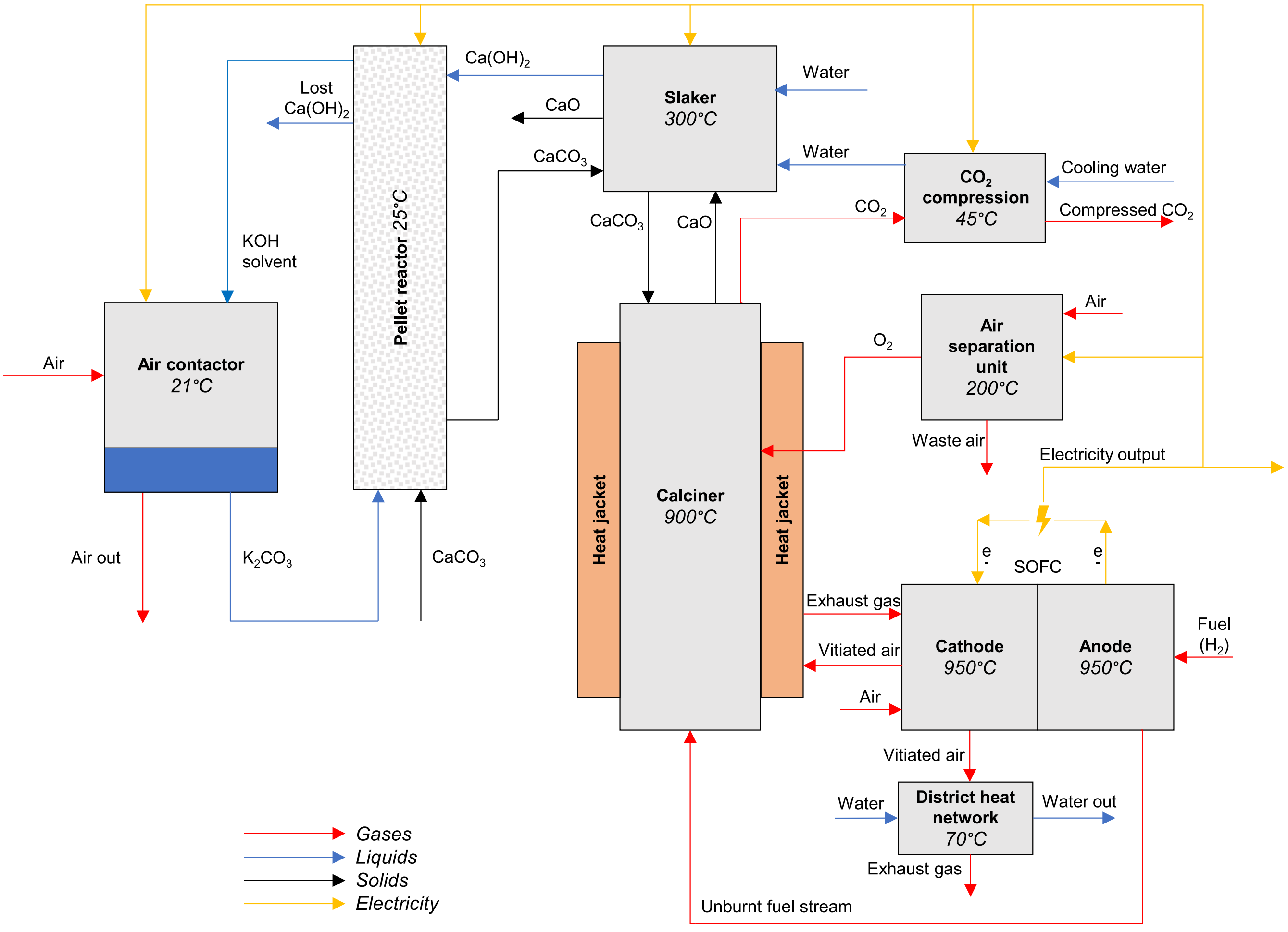

Fig. 1. Block diagram of DAC-SOFC system.

(KOH) solution to form potassium carbonate (K_2CO_3), as presented in Eq. (1). This solution is pumped into the pellet reactor, which contains calcium carbonate ($CaCO_3$) pellets suspended in a solution flowing upwards through the reactor. A slurry of calcium hydroxide ($Ca(OH)_2$) is injected at the bottom of the reactor from slaker, driving the dissolution of $Ca(OH)_2$ and the precipitation of $CaCO_3$, as presented in Eq. (2). Small seed $CaCO_3$ pellets are formed at the top of pellet reactor. As they grow in size, they discharge from the bottom of the reactor to the calciner, where $CaCO_3$ is thermally decomposed at approximately 900 °C to yield CO_2 and calcium oxide (CaO), as presented in Eq. (3). The CO_2 stream is then compressed and cooled in the compression unit, ready to be sequestered or sold and transported. In the slaker unit, CaO is hydrated to form $Ca(OH)_2$, which can then be fed back into the pellet reactor, as presented in Eq. (4). The balance equations detailed in the process are summarised below [6].

$$2KOH + CO_2 \rightarrow K_2CO_3 + H_2O \tag{1}$$

$$K_2CO_3 + Ca(OH)_2 \rightarrow 2KOH + CaCO_3 \tag{2}$$

$$CaCO_3 \rightarrow CaO + CO_2 \tag{3}$$

$$CaO + H_2O \rightarrow Ca(OH)_2 \tag{4}$$

3.2. Solid oxide fuel cell

The SOFCs are fuel cells with dense ceramic electrolyte transporting oxygen ions and filling the space between the electrodes material, operating at 600–1,200 °C [41]. The overall chemical reaction of the hydrogen fed SOFC combines hydrogen with oxygen to form water, as presented in Eq. (5). This can be divided into two half reactions: at the cathode, oxygen ionises to form O^{2-}, as shown in Eq. (6); and at the anode, a gaseous hydrogen molecule is oxidised to form a water molecule whilst releasing electrons, as shown in Eq. (7) [23].

$$H_2 + \frac{1}{2}O_2 \rightarrow H_2O \tag{5}$$

$$\frac{1}{2}O_2 + 2e^- \rightarrow O^{2-} \tag{6}$$

$$H_2 + O^{2-} \rightarrow H_2O + 2e^- \tag{7}$$

The electrons flow between the anode and cathode via an external electrical circuit, generating DC electricity (which can be converted to AC with an additional converter not modelled in this study). In this study, electricity generated from SOFC supplies power to the fan and pump in the air contactor, the fluid pump in the pellet reactor, the slaking process in slaker, the air separation unit, and the CO_2 compression system. At the anode, high temperature exhaust gas is released containing excess fuel and steam, while at the cathode, off-gas is released containing vitiated air from which oxygen has been separated out [39]. Anode materials should cover a large surface area of triple phase boundary to maximise the anodic reaction and should also have prominent porous microstructure to facilitate a quick fuel gas transport. The metal-based materials with characteristics of high electrocatalytic activity for fuel oxidation and high ionic and electronic conductivity, such as nickel-yttria stabilised zirconia (Ni-YSZ), were investigated as potential anode materials [41]. High temperature and high utilisation of fuel gas in the cell anode will increase a risk of re-oxidation of Ni, which will damage the cell [42]. As AspenPlus cannot model the flow of electrons, the model for the SOFC was approximated to simulate the overall reaction as Eq. (5). Neither bypass side reaction nor re-oxidation reaction is considered in this model.

The rated power of SOFC ($\dot{W}_{SOFC,DC}$) is specified as 50 $MW_{el,\ dc}$, which is used as an input in the model to calculate the total area of the SOFC stack (AC_{SOFC}) using Eq. (8) [43]:

$$\dot{W}_{SOFC,DC} = V_{SOFC} \times I_C \times AC_{SOFC} = V_{SOFC} \times I_{SOFC} \tag{8}$$

where V_{SOFC} is voltage of SOFC, I_C is current density, and I_{SOFC} is the current generated by the SOFC and can be calculated by Eq. (9) [44]:

$$I_{SOFC} = zn_{H_2}F \tag{9}$$

where z is the number of electrons transferred per reaction, i.e., 2 in this study, n_{H_2} is the mole flow rate of reacted H_2, and F is Faraday constant, 96,485 A•s/mol. In the base case design of this study, a given current density (210 mA/cm^2) from [39] is used.

Calculation of voltage of SOFC is built based on the Nernst voltage and semi-empirical models for multiple deviation of voltages. These equations are organised in Table 2 and implemented in AspenPlus using a *design spec* Fortran block function.

where $\Delta\overline{g_f}$ is molar Gibbs free energy change for the H_2 electrochemical reaction, and R = 8.314 J/(mol•K) [49]. Moreover, T_{SOFC}, T_{ref}, P_{SOFC}, and P_{ref} are operating and reference temperature and pressure for SOFC, respectively. In Eq. 11, 0.008 is the constant when operating temperature in the range 900 °C-1,050 °C [48]. In Eq. 12, 76 stands for theoretical Nernst constant (mV/decade) [48]. In Eq. 13, 172 is the theoretical Nernst constant (mV/decade) [48], $\frac{P_{H2}}{P_{H2O}}$ is the ratio of H_2 and steam partial pressures in the system, and $\left(\frac{P_{H2}}{P_{H2O}}\right)_{ref}$ is the ratio of H_2 and steam in the system under reference conditions. In Eq. 14, 92 is the theoretical Nernst constant (mV/decade) [48], P_{O2} and P_{O2ref} are the oxygen partial pressures in the system for the actual case and the reference case, respectively. Table 3 lists base case design parameters.

3.3. Integrated solid oxide fuel cell-calciner setup

The critical part of this process is the calcination setup, which was modelled based on the natural gas fed system [8] and adjusted for a SOFC unit fed by pure hydrogen. The SOFC's cathode exhaust gases consist of vitiated air, and the anode exhaust consists of unburnt hydrogen fuel and steam, both at 950 °C. The anode exhaust is fed directly to the calciner where the unburnt hydrogen based on the fuel utilisation factor and steam from the SOFC is combusted, providing the heat required for calcination through direct transfer. Pure oxygen from

Table 2
Voltage equations of the SOFC.

Parameters	Equations		References
The Nernst voltage (Standard operating condition voltage), V_{ref} [a]	$V_{ref} = -\frac{-\Delta\overline{g_f}}{2F} + \frac{RT_{ref}}{2F} ln\left[\frac{P_{H_2}(P_{O_2})^{0.5}}{P_{H_2O}}\right]$	(10)	[45,46]
Voltage changes due to operating temperature and current density, ΔV_T [a]	$\Delta V_T = 0.008 \times (T_{SOFC} - T_{ref}) \times I_C$	(11)	[47,48]
Voltage changes due to operating pressure, ΔV_p [b]	$\Delta V_p = 76 \times \log\left(\frac{P_{SOFC}}{P_{ref}}\right)$	(12)	[47,48]
Voltage changes due to fuel composition, ΔV_{anode} [c]	$\Delta V_{anode} = 172 \times \log\left[\frac{\frac{P_{H2}}{P_{H2O}}}{\left(\frac{P_{H2}}{P_{H2O}}\right)_{ref}}\right]$	(13)	[47,48]
Voltage changes due to oxidant composition, $\Delta V_{cathode}$ [d]	$\Delta V_{cathode} = 92 \times \log\left(\frac{P_{O2}}{P_{O2ref}}\right)$	(14)	[47,48]
Actual output voltage of the SOFC,V_{SOFC}	$V_{SOFC} = V_{ref} + \Delta V_T + \Delta V_p + \Delta V_{anode} + \Delta V_{cathode}$	(15)	[47,48]
[a] $T_{ref} = 1{,}000$ °C, [b] $P_{ref} = 1$ bar, [c] $\left(\frac{P_{H2}}{P_{H2O}}\right)_{ref} = 0.15$, [d] $P_{O2ref} = 0.164$.			[39]

Table 3
Base case design conditions and model assumptions.

Parameter		Value	Reference
SOFC	Rated power output ($MW_{el,\ dc}$)	50	–
	AC-DC conversion efficiency (%),$\eta_{AC/DC}$	96	[39]
	Operating pressure (bar),P_{SOFC}	1.08	[39]
	Operating temperature (°C),T_{SOFC}	950	[8]
	Reference voltage (mV),V_{ref}	700	[39]
	Current density (mA/cm^2),I_C	210	[39]
	Fuel utilisation (–),U_f	0.60	[39]
	Fuel composition	Pure hydrogen	–
Calciner	Operating temperature (°C)	900	[6]
	Air separation unit specific power requirement (kWh/tO$_2$)	262	
	Operating pressure (bar)	1.0	
	$CaCO_3$ conversion efficiency (%)	98	
Contactor	Fan energy (kWh/tCO$_2$)	67	[6]
	Fluid pumping energy (kWh/tCO$_2$)	23	
	Aqueous solution composition	1.0 M OH^-, 0.5 M CO_3^{2-}, 2.0 M K^+	
	Fraction of CO_2 captured (%)	75	
Pellet Reactor	Calcium retention	0.9	[6]
	Fluid pumping energy (kWh/tCO$_2$)	39	
Slaker	Power required by slaking heat (kWh/tCO$_2$)	35	[6]
	Conversion to CaO	0.85	
Auxiliary	Compressor power usage (kWh/tCO$_2$)	14	[6]
	CO_2 purity (%$_{mass}$)	83	
	CO_2 pressure (bar)	150	

air separation unit is input to the calciner for the full combustion of hydrogen. The flow rate of hydrogen fed to the SOFC is adjusted by *design spec* Fortran block function in AspenPlus to achieve the rated power output of 50 $MW_{el,\ dc}$. As the cathode exhaust is not suitable for combustion, it is fed to a heat jacket surrounding the calciner, providing additional heat via indirect heat transfer. The cathode exhaust gas is then recirculated, preheating the ambient air entering the SOFC via a heat exchanger, and then passing through to another heat exchanger, where the remaining heat can be used to heat water to 70 °C, to be sent to a district heat network. The details of setup of SOFC and calciner in AspenPlus are described in **Supplementary Information S.1**.

3.4. *Thermodynamic assumptions*

Table 3 details the key thermodynamic assumptions made in the AspenPlus model. A 50 $MW_{el,\ dc}$ SOFC was selected to provide the high-grade heat and electricity, as it would have sufficient capability to provide the magnitude of heat and power required to conduct an L-DAC process in the range of thousand tonne of CO_2 per year. Additionally, SOFCs in the range of 1–60 $MW_{el,\ dc}$ are comparable to existing combined heat and power plants [50]. As the air separation unit wasn't modelled in this study, its power requirement was cited from Keith et al. [6], i.e., 262 kWh/tO$_2$. Fraction of CO_2 captured (75 %) at air contactor is cited from Keith et al. [6], which has been validated by pilot data.

The fuel utilisation of the SOFC (U_f) is defined as the molar proportion of fresh fuel fed to the SOFC that is used in the SOFC's electrochemical reactions (i.e., the remaining proportion of the fresh fuel is released via the exhaust). In line with [39], a U_f of 0.6 was set as the base case for the proposed model based on preliminary testing to achieve increased levels of thermal decomposition of $CaCO_3$ in the L-DAC process. The air utilisation of the SOFC (U_a) is defined as the fraction of the consumed oxygen ($n_{O_2,consumed}$) to the input oxygen ($n_{O_2,in}$) at cathode, which can be calculated as Eq. (16).

$$U_a = \frac{n_{O_2,consumed}}{n_{O_2,in}} \tag{16}$$

Referring Stefano's work [48], $n_{O_2,consumed}$ can be calculated by Eq. (17):

$$n_{O_2,consumed} = \frac{I_C \times AC_{SOFC}}{4F} \tag{17}$$

where air utilisation factor is calculated as 0.14 based on the base case design conditions.

An important aspect of the overall setup that must be noted for thermodynamic analysis is that the system was specified in AspenPlus to maintain a 98 % conversion rate of $CaCO_3$ and an output temperature from the calciner of 900 °C. These specifications were met by adjusting the hydrogen fuel supplied to the SOFC, and by extension of the hydrogen supplied to the calciner at a specified value of U_f. As the thermal decomposition of $CaCO_3$ is an endothermic reaction, the amount of hydrogen fuel must be controlled in order for the reaction to be maintained at 900 °C.

3.5. *Economic assumptions*

A combination of economic estimations and assumptions were used to calculate the capital expenditure (*CapEx*) and operating expenditure (*OpEx*) of the proposed system, as well as to establish the widely used techno-economic performance indicator for DAC. In the integrated system, the price of hydrogen (C_{fuel}) as a fuel cost will impact the results of *LCOA*. Prices of hydrogen produced through electrolysis using renewable energy sources are fundamentally linked to renewable electricity prices. The electricity market is volatile and currently prices are high due to fuel supply constraints and uncertainty [51]. In this study, it was assumed that a power purchase agreement (PPA) of renewable electricity for hydrogen generation via electrolysis has been established. Extra cost for hydrogen storage and transportation was not included. Table 4 details current hydrogen prices in the UK based on PPAs. The base case applied the lowest cost option of hydrogen, i.e., generated with electricity from an offshore wind PPA. Due to the current elevated price of hydrogen production and the widely anticipated fall in prices with increased investment, C_{fuel} was modelled with the consideration of a gradual decline in production cost over time [51]. Therefore, it was assumed that a new PPA would be negotiated every 5 years and the price of hydrogen would go down by 10 % each time to reflect the possibility of making slow progress on these targets.

Scaling estimates for the *OpEx* and *CapEx* of the system are made in Table 5. The L-DAC component prices primarily were scaled linearly. As the air contactor and pellet reactor are modular, when scaling down, their capital cost would be consistent to a minimum capacity of 91 ktCO$_2$/year [6]. However, the calciner unit would be the exception (as it was a bespoke unit), therefore its costs were not scaled linearly. This was accounted for when calculating costs; the conservative assumption was made by applying an 80 % increase to the capital costs of this unit if the capacity of the model was less than half of 907 ktCO$_2$/year [6]. A regular replacement of SOFC is considered on a 5-year basis within the project lifetime, of which the expenses correspond to 25 % of the total capital costs of SOFC [53]. Other key economic parameters utilised in the

Table 4
Hydrogen Prices.

Levelised Cost of Hydrogen	Value	Reference
Offshore wind PPA based hydrogen (£/kg)	7.83	[52]
Onshore wind PPA based hydrogen (£/kg)	8.34	[52]
Solar PPA based hydrogen (£/kg)	10.73	[52]
Renewable electrolysis based hydrogen in 2050 (£/kg)	1.50	[51]

Table 5
Economic costing and scaling assumptions.

Capital and Operating Expenditures Scaling Breakdown			Value	References
Direct air capture process	Field CapEx	Air contactor system (£/tCO_2)	173	[6]
		Pellet reactor (£/tCO_2)	107	
		Calciner and slaker units (£/tCO_2)*	64	
		Air separation unit (£/tCO_2)	44	
		CO_2 compressor (£/tCO_2)	16	
		Fines filter (£/tCO_2)	25	
		Other equipment (£/tCO_2)	84	
		Buildings (£/tCO_2)	5	
		Transformer (£/tCO_2)	16	
		Indirect field costs (£/tCO_2)	72	
		Total field costs (£/tCO_2)	607	
	Non-field CapEx	Engineering (£/tCO_2)	110	[6]
		Other project costs (£/tCO_2)	39	
		Contingency (£/tCO_2)	128	
		Total non-field costs (£/tCO_2)	277	
	Total CapEx	$CapEx_{DAC}$(£/tCO_2)	885	[6]
	OpEx	Annual fixed and variable costs**, $OpEx_{DAC}$(£/tCO_2)	34	[6]
Solid oxide fuel cell	CapEx	SOFC stack (£) [Area, AC_{SOFC} (m^2); Operating temperature, T_{SOFC} (K)]	$C_{SOFC} = AC_{SOFC}(2.96T_{SOFC} - 1907)$	[8]
		DC-AC inverter (£) [Rated power output, $\dot{W}_{SOFC,DC}$(kW_{el})]	$C_{SOFC,DC/AC} = 10^5 \times \left(\frac{\dot{W}_{SOFC,DC}}{500}\right)^{0.7}$	
		SOFC auxiliaries (£)	$C_{SOFC,aux} = 0.1C_{SOFC}$	
		Total SOFC CapEx, $CapEx_{SOFC}$(£)	$CapEx_{SOFC} = C_{SOFC,aux} + C_{SOFC,DC/AC} + C_{SOFC}$	
		Air preheater (£) [Heat exchanger area, AC_{HX1}(m^2)]	$C_{HX1} = 130\left(\frac{AC_{HX1}}{0.093}\right)$	
		District heat exchanger (£) [Heat exchanger area, AC_{HX2} (m^2)]	$C_{HX2} = 130\left(\frac{AC_{HX2}}{0.093}\right)$	
		SOFC stack cost in 2050 ($/$kW_{dc}$)	207	[54]
	OpEx	Annual fixed costs (£)	$OpEx_{SOFC,fixed} = 0.01CapEx_{SOFC}$	[8]
		Annual variable costs (£)	$OpEx_{SOFC,var} = 0.02CapEx_{SOFC}$	
		Total annual operating costs, $OpEx_{SOFC}$ (£)	$c = 0.03CapEx_{SOFC}$	
	Replacement cost	Replacement cost of SOFC every 5 years within project lifetime (£)	$C_{SOFC,rep} = 0.25CapEx_{SOFC}$	[53]
Fuel costs		Hydrogen price for base case, C_{fuel} (£/kg)	7.83	[52]
		Reduction in hydrogen price (%/5 years)	10	–

[*] The capital cost / unit capacity would be ~ 80 % larger than this figure for systems smaller than 907 ktCO_2/year [6].

[**] Fixed costs would dominate the operating expenditure, therefore the number was quoted as an overall figure.

calculation of levelised costs are presented in Table 6.

3.6. Modelling of key performance indicators

A selection of key performance indicators (KPIs) was used to assess the performance of the DAC-SOFC system for CO_2 capture and power generation capabilities. The energy balance of the SOFC system is evaluated based on Eq. (18). An assumption was made for the SOFC, i.e., as the operation of the SOFC stack was isolated, there was no heat exchange between the system and its surrounding environment. The energy losses from SOFC were accounted in terms of the heat involved in the anode and cathode exhausts and the unburnt hydrogen at the anode, all of which were recovered and used in the calcination process.

Table 6
Assumptions of project deployment.

Parameter	Value	Reference
USD-GBP exchange rate – March 2023	0.83	[55]
Project lifetime (years)	25	[8]
Capacity factor (%)	80	[8]
Fuel cell degradation rate (mV/1000hrs)	5	[8]
Loan interest rate (%)	5	[8]
Internal rate of return (%)	8.78	[8]
Owners' equity share (%)	50	–
Proportion of debt (%)	50	–
Price of electricity (£/$MW_{el}h$)	120	[56]
Carbon price – UK 2023 (£/tCO_2)	44	[57]

$$\dot{m}_{fuel}LHV_{fuel} = \dot{E}_{calciner} + \dot{W}_{SOFC} + \sum(\dot{m}h)_{out,other} - \sum(\dot{m}h)_{in,other} \tag{18}$$

where $\dot{m}_{fuel}$ is mass flow rate of fuel supplied to SOFC, LHV_{fuel} is the lower heating value of the fuel, $\dot{E}_{calciner}$ is energy supplied to the calciner which includes the heat and unburnt fuel from anode exhaust to the calciner and heat from cathode exhaust to a heat jacket surrounding the calciner, $\dot{W}_{SOFC}$ is power output from SOFC which equals $\dot{W}_{SOFC,DC}$ multiplied by AC-DC conversion efficiency ($\eta_{AC/DC}$), and $\sum(\dot{m}h)_{out,other} - \sum(\dot{m}h)_{in,other}$ is enthalpy changes of other input and output flows to the SOFC. The $\dot{E}_{calciner}$ is calculated as Eq. (19):

$$\dot{E}_{calciner} = \dot{m}_{excess}LHV_{fuel} + \dot{m}_{steam}(h_{steam,in} - h_{steam,out}) + \dot{m}_{cath}(h_{cath,in} - h_{cath,out}) \tag{19}$$

where $\dot{m}_{excess}$, $\dot{m}_{steam}$, $\dot{m}_{cath}$ are the mass flow of unburnt fuel, steam, and cathode exhaust, respectively, and $h_{steam,in}$, $h_{steam,out}$, $h_{cath,in}$, $h_{cath,out}$ are input and output specific enthalpy of steam and cathode exhaust, respectively.

The calciner setup for this system was indicative of the validity of the process setup, and therefore the specific energy consumption of the calciner ($\dot{q}_{calciner}$), as defined in Eq. (20), was used for validation purposes with other models:

$$\dot{q}_{calciner} = \frac{\dot{E}_{calciner}}{\dot{m}_{CO2,out} - \dot{m}_{CO2,in}} \tag{20}$$

where the lower part of Eq. (20), $\dot{m}_{CO2,out} - \dot{m}_{CO2,in}$, is the mass flow rate of production of CO_2 in the calciner.

The net power output of the integrated DAC-SOFC system ($\dot{W}_{net}$) is estimated by Eq. (21):

$$\dot{W}_{net} = \dot{W}_{SOFC} - \dot{W}_p \tag{21}$$

where $\dot{W}_p$ is the DAC process' parasitic load which is calculated by Eq. (22):

$$\dot{W}_p = M_{DAC} \times (\dot{W}_{cal} + \dot{W}_{fan} + \dot{W}_{pump} + \dot{W}_{sla} + \dot{W}_{com}) \tag{22}$$

where M_{DAC} is DAC capacity, and $\dot{W}_{cal}$, $\dot{W}_{fan}$, $\dot{W}_{pump}$, $\dot{W}_{sla}$, and $\dot{W}_{com}$ are specific power consumption for calciner unit, fan, fluid pumps, slaker, and CO_2 compressors, respectively, which are given in Table 3.

The net system efficiency (η_{net}) of whole integrated system is a measure of how effective the system is at delivering excess electricity for sale, as defined by Eq. (23):

$$\eta_{net} = \frac{\dot{W}_{net}}{\dot{m}_{fuel} LHV_{fuel}} \tag{23}$$

where $\dot{m}_{fuel}$ is mass flow rate of fuel supplied to solid oxide fuel cell. The thermal efficiency of SOFC (η_{SOFC}), as defined in Eq. (24), is a measure of the fuel cell's ability to deliver power given a chemical input:

$$\eta_{SOFC} = \frac{\dot{W}_{SOFC}}{\dot{m}_{fuel} LHV_{fuel}} \tag{24}$$

The *LCOA* represents the real cost of air capture accounting for the discounted sum of costs over the system's lifetime, divided by the discounted amount of carbon captured over the plant's lifetime, as detailed in Eq. (25) [8]. The LCOE was calculated similarly in Eq. (26), using the discounted costs of the system and the discounted production of electricity. These equations are estimated for the entire DAC-SOFC system, which means that the costs of both DAC and SOFC systems contribute to the total *CapEx* and *OpEx*. The *LCOA* and the *LCOE* therefore indicate the price at which either CO_2 or net electricity would have to be sold as a product for the integrated system to break even, assuming that the price of the other would remain at zero [8].

$$LCOA = \frac{\sum_{t=0}^{n} \frac{I_t + LR + OpEx + 8760\dot{m}_{fuel} C_{fuel} k}{(1+i)^t}}{\sum_{t=0}^{n} \frac{8760\dot{m}_{co2} k}{(1+i)^t}} \tag{25}$$

$$LCOE = \frac{\sum_{t=0}^{n} \frac{I_t + LR + OpEx + 8760\dot{m}_{fuel} C_{fuel} k}{(1+i)^t}}{\sum_{t=0}^{n} \frac{8760\dot{W}_{net} k}{(1+i)^t}} \tag{26}$$

where I_t is the investment cost in year *t*, *LR* is the annual debt service, *OpEx* is the annual operating expenditure, (which would be dominated by fixed costs and therefore was not adjusted with the capacity factor, *k*). The mass flow rate of fuel ($\dot{m}_{fuel}$) was adjusted by capacity factor *k*, the number of hours in a year i.e., 8,760 h, and the price of hydrogen in year *t* ($C_{fuel,t}$). The sum of these costs was discounted by the internal rate of return (*i*) for each year of the project's lifetime (*n*). The discounted sum of costs was divided by the discounted sum of CO_2 captured ($\dot{m}_{CO2}$) and the electricity generated ($\dot{W}_{net}$), respectively.

4. Results and discussion

In this section, the performance of the proposed DAC-SOFC integrated system is firstly evaluated and compared with the performance of two referenced systems. The effects of fuel utilisation of the SOFC on the integrated system are studied in terms of the energy consumed by the calciner, the capture capacity of the system, and thermal and economic results. A future scenario is created to analyse cost distribution of the system in 2050.

4.1. Comparison of key performance indicators

To validate the model of SOFC developed in this study, the results obtained from the current SOFC model are compared with the simulation work by Zhang et al. [39]. The fuel composition used in the Zhang et al.'s model includes 81.3 % CH_4, 2.9 % C_2H_6, 0.4 % C_3H_8, 0.2 % C_4H_{10}, 14.3 % N_2, and 0.9 % CO, with a fuel utilisation factor of 85 %. Fig. 2 compares the results from the current SOFC model, the referenced work, and reference voltage obtained from Eq. 10, which demonstrates a similar decreased trend in voltage changes with current density. The higher voltage in present study is triggered by the lower operating temperature of 980 °C compared to that in Zhang et al. (1,000 °C), leading more significant voltage changes (ΔV_T) due to the corresponding operating temperature and current density. The model of L-DAC is consistent with the model created by Bianchi et al.'s work [40]. Their model has been validated previously with CE's pilot data [6].

Table 7 details the KPIs for both the thermodynamic and economic performance of the DAC-SOFC integrated system. It can be noted that, as CE's [6] system is solely an L-DAC plant, with no power generation capabilities, there are a significant number of KPIs that are not applicable to it. However, the CE's [6] system remains present for validation purposes, as the L-DAC process used in the proposed system is based upon their model.

For a U_f of 0.6, the proposed DAC-SOFC system delivers a maximum capacity of 270 ktCO$_2$/year. An estimated 37.6 MW$_{th}$ of thermal energy generated was supplied to the calciner via heat transfer from the SOFC's exhaust gases. The parasitic load ($\dot{W}_p$) of the L-DAC was 17.3 MW$_{el}$, with an excess 28.7 MW$_{el}$ generated by the SOFC, which could be sold to the grid. This system resulted in an *LCOA* and *LCOE* of £1,013/tCO$_2$ and £1,127/MW$_{el}$h, respectively, compared to the current rates of approximately £44/tCO$_2$ and £120/MW$_{el}$h detailed in Table 6. As its CO_2 capture capacity is over a quarter of the CE's system [6], it sits firmly above the 91 ktCO$_2$/year benchmark and confirms that the economic scaling assumptions made in Table 5 are valid.

The calciner energy consumption, $\dot{q}_{calciner}$, is not a traditional KPI for such processes, but was chosen to technically validate the setup of the calciner in the model, as this is the critical aspect that differs in the proposed model compared to the established CE's setup of the system [6]. The identical $\dot{q}_{calciner}$ of 4.40 GJ/tCO$_2$ confirms the modelling of the calciner is correct for the system given. It must be acknowledged that $\dot{q}_{calciner}$ for the Hanak et al.'s [8] system is almost half that of the CE's system [6]. One potential reason for the lower $\dot{q}_{calciner}$ could be that the CO_2 leaving the calciner in the model was set at a temperature of ~ 500 °C, despite operating temperature of the calciner remaining at

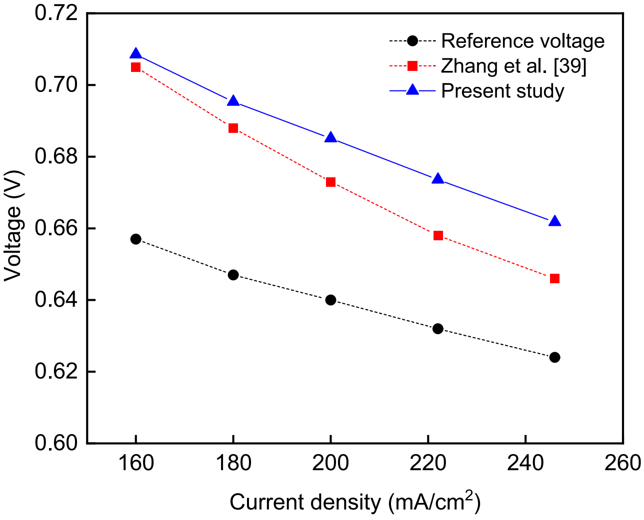

Fig. 2. Validation of SOFC model in this study.

Table 7
Comparison of KPIs between proposed system and reference systems [6,8].

Variety	Parameter	Proposed system	Hanak et al.'s system [8]	CE's system [6]
Thermodynamic	Plant capture capacity (tCO_2/year)	269,317	182,385	901,600
	Fuel type	Hydrogen	Natural Gas	Natural Gas
	Calciner energy consumption, $\dot{q}_{calciner}$ (GJ/tCO_2)	4.40	2.51*	4.41*
	Power output, $\dot{W}_{SOFC}$ (MW_{el})	46.0	24.2	–
	Net power output, $\dot{W}_{net}$ (MW_{el})	28.7	21.3	–
	Parasitic load, $\dot{W}_p$ (MW_{el})	17.3	2.9	–
	Thermal energy supply to calciner, $\dot{Q}_{calciner}$ (MW_{th})	37.6	–	–
	Thermal efficiency of SOFC, η_{SOFC} ($\%_{LHV}$)	42.2	46.8	–
	Net system efficiency, η_{net}($\%_{LHV}$)	24.2	47.7	–
	Fuel utilisation of SOFC, U_f(−)	0.60	0.85	–
	H_2 consumption (t/tCO_2)	0.113	–	–
	Operational voltage of SOFC, V_{SOFC} (V)	0.68	0.70	–
Economic	Levelised cost of capture, *LCOA* (£/tCO_2)	1,013	149*	123–304*
	Levelised cost of electricity, *LCOE* (£/MW_{el}h)	1,127	50	–
	Cost of fuel** (£/GJ)	65.17	3.50	2.59

* The figure is stated to account for the net CO_2 removed from the atmosphere.

** Unlike in Table 5, the price of fuel is measured in £/GJ to compare the energy provided as LHV values of fuels differ.

900 °C. Another possible reason is that the calciner in the Hanak et al.'s [8] system was governed by electrochemistry specified in an alternative Excel file (which is not freely accessible). With the limited information provided, the model could not be recreated accurately, and therefore only speculation can be made as to the reasons for the divergence in their results.

The proposed model's net efficiency (η_{net}) is significantly lower than that of the Hanak et al.'s [8] system, which reflects the larger parasitic load ($\dot{W}_p$) of the DAC system in this model. Hanak et al. [8] utilises an alternative once-through DAC concept, where $CaCO_3$ is fed directly to calciner and the thermally decomposed products of CaO and CO_2 are both sold, with no regeneration cycle for the CaO, as is the case in CE's [6] model and the one proposed in this study. The once-through DAC process has lesser power demands, as smaller quantities of fluid must be pumped around the system and pressurised, hence the DAC system has a lower parasitic load.

Additionally, Hanak et al [8] modelled the system as a combined DAC and power generation plant, whereas the proposed model for this study must be considered more alike to the CE's model [6], with the primary purpose of conducting DAC, and the added benefit in the proposed model of generating additional revenue through selling excess electricity and heat. This justifies the lower η_{net}, as it is anticipated in the proposed model that $\dot{W}_p$ will dominate the power generation capabilities of the SOFC. While naturally it is still beneficial to minimise the parasitic load ($\dot{W}_p$), the nature of a regenerative system is more energy intensive than a once-through system but comes with the economic benefit of recycling material and an inherent sustainability.

Similarly, the *LCOE* of £1,127/MW_{el}h being two orders of magnitude higher than the Hanak et al.'s [8] system, while unhelpful economically for the proposed system, is not an indicator of the model's inaccuracy. The value of *LCOE* as detailed in Eq. (26) assumes that the primary income stream of the proposed system (carbon capture) does not exist and is instead covering costs entirely with revenue generated from selling electricity generated. Hanak et al. [8] proposed a combined power generation and carbon capture plant, and therefore is analysing two comparable income streams with this method of *LCOE*. However, the proposed system here is geared towards its primary purpose of performing L-DAC, which means that the objective of the plant is to maximise its carbon capture capabilities, rather than its η_{net}, which would otherwise help the SOFC system generate more excess electricity.

Both *LCOA* figures in Hanak et al.'s [8] and CE's [6] systems account for the fact that they burn natural gas to power DAC, and therefore release additional carbon into their respective systems, by subtracting the amount of CO_2 released as a result of combustion from the final carbon output figures of the system (this figure is often referred to as the net CO_2 removed from the atmosphere). The proposed system's *LCOA* at £1,013/tCO_2 is significantly higher than other two systems, as well as being higher than the estimates predicted across literature on the subject, which typically state a maximum of around £915/tCO_2 [10]. Fig. 3 shows the distribution of *CapEx* and *OpEx* for the integrated DAC-SOFC system. In total, the *CapEx* is £303.27 million, the *OpEx* excluding fuel is £21.43 million, and the fuel costs is £194.70 million. The *CapEx* accounts for 58 % of total expenses for the integrated system, followed by fuel costs at 37 %. Excluding fuel costs, fixed and variable *OpEx* represent only 1.9 % and 0.15 % of the total costs, respectively. It demonstrates that the system's *OpEx* is heavily dominated by fuel costs, as the price of hydrogen used in the proposed model is approximately 20 times the price of the fuels used in Hanak et al.'s [8] and CE's [6] systems. However, as Table 4 indicates, this cost is anticipated to drop dramatically as increasing investment is made in hydrogen production. It is also a reasonable assumption that given the global push towards net zero targets, the availability and price of natural gas will eventually render the combustion of fossil fuels economically inviable.

4.2. *Thermodynamic and economic results*

Using a fixed 50 $MW_{el,\ dc}$ SOFC to provide both heat and electricity to the L-DAC system means that the amount of CO_2 captured depends on the thermal energy delivered by the SOFC to the calciner, both directly and indirectly via the exhaust gases of the calciner. The energy available to the calciner varies with the U_f of the SOFC, as demonstrated in Fig. 4a. The heat transferred via the heat jacket, i.e., from the cathode exhaust, remains relatively constant (due to the air requirements for the SOFC remaining largely similar despite U_f variation) while the energy via combustion declines almost linearly with U_f. As U_f increases in the SOFC, less fuel is sent to the calciner and therefore less fuel is combusted there, and the thermal energy provided for the decomposition of $CaCO_3$ declines.

The capacity of the system to remove CO_2 is dictated by the energy available from the SOFC's exhaust gases to maintain a 98 % conversion rate of $CaCO_3$ delivered to the calciner, and to maintain the required calcination temperature of 900 °C. The power requirements of the DAC process (i.e., the parasitic load $\dot{W}_p$) decline linearly with the capacity of the DAC plant, as the parameters in Table 3 set out. Fig. 4b demonstrates this, as the plant capacity and $\dot{W}_p$ steadily decline together while the U_f of the SOFC increases. Decline in the plant capacity also increases specific energy consumption of calciner, as shown in Fig. 4c, where energy required for separating one tonne of CO_2 from $CaCO_3$ increases from 4.40 GJ/tCO_2 to 5.53 GJ/tCO_2 with the increase of the U_f. Even though the energy supplied by the SOFC to the calciner decreases as the U_f increases, the higher U_f can result in a more significant reduction in the plant capacity.

Fig. 4d indicates that η_{SOFC} peaks at ~ 0.77, showing that the SOFC's

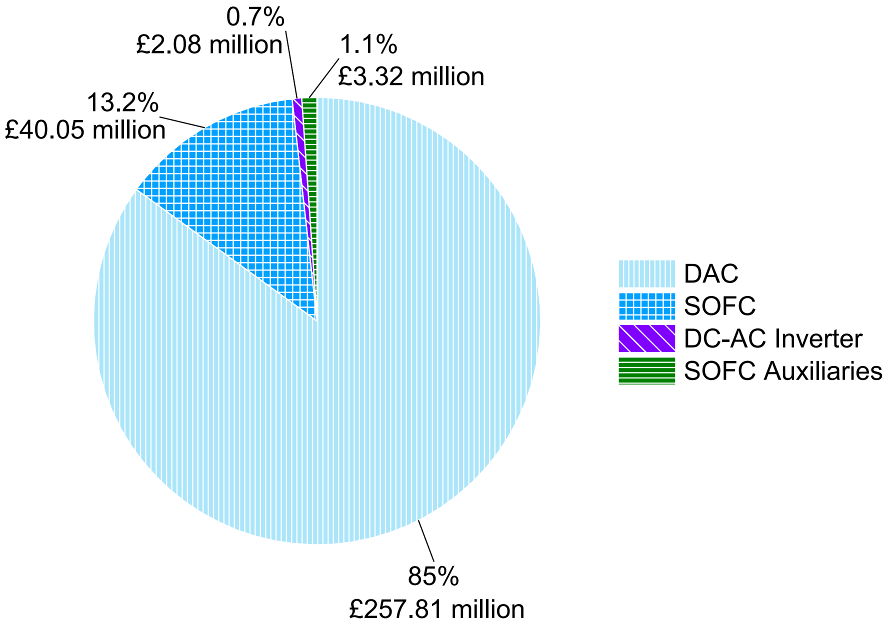

(a) CapEx distribution

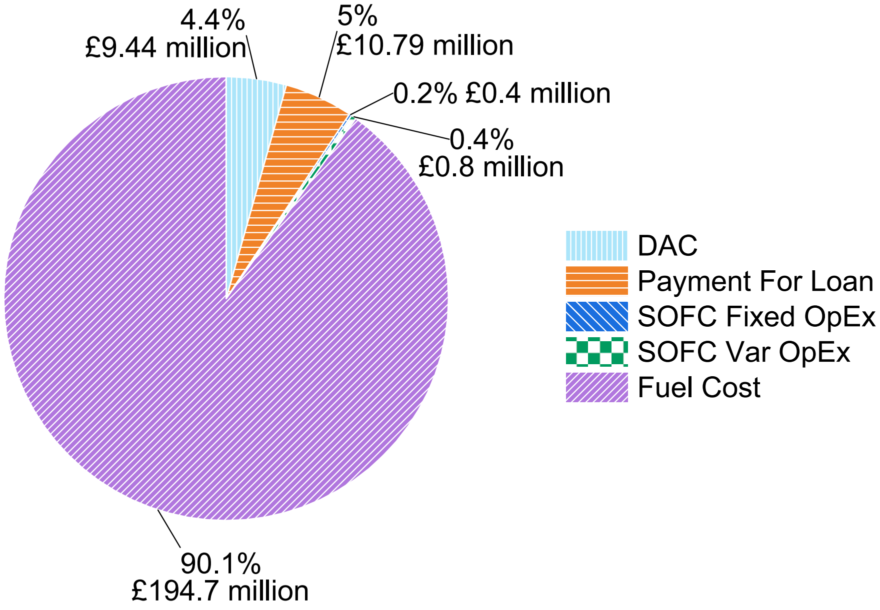

(b) OpEx distribution

Fig. 3. Initial cost distribution of proposed model.

power generation is most efficient at this point. However, η_{net} decreases at a slower rate and appears to level off with increasing U_f. This can be explained referring to Fig. 4b, as the plant capacity and thus $\dot{W}_p$ continue to decline with U_f. This is because the amount of $CaCO_3$ that can be thermally decomposed while maintaining a 98 % conversion rate of $CaCO_3$ and a temperature in the calciner of 900 °C declines as less fuel and heat is delivered to the calciner by the SOFC. Therefore, $\dot{W}_{net}$ continues to increase with U_f, as this figure is simply the rated 50 $MW_{el,\ dc}$ output converted to AC ($\dot{W}_{SOFC}$), less $\dot{W}_p$.

The *LCOA* of the system in Fig. 4e is dominated by the cost of hydrogen fuel and therefore minimised when the fuel is utilised most effectively between both the calciner and the SOFC. Conversely, the

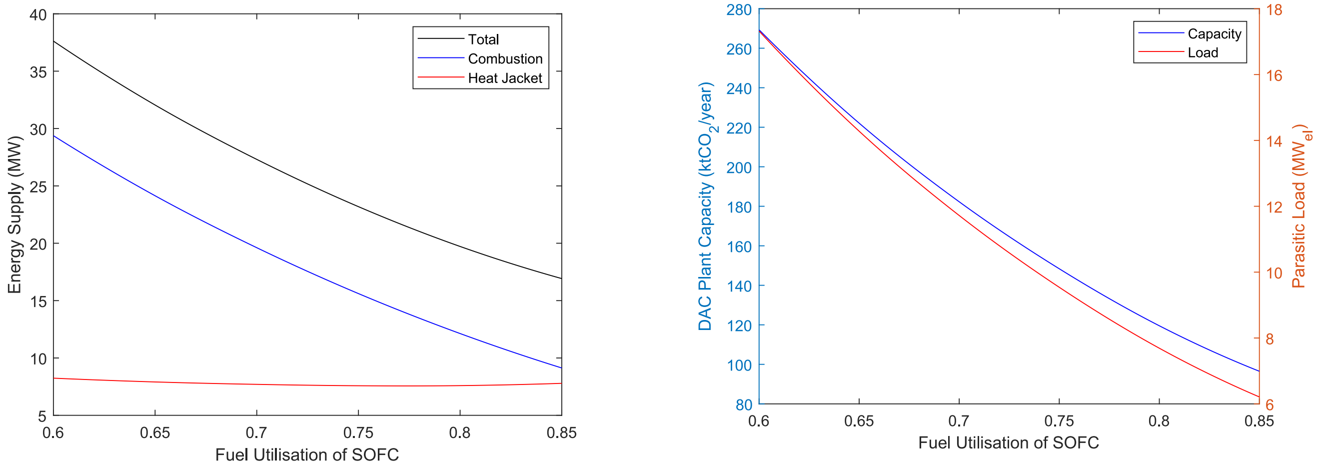

(a) Energy supplied to calciner

(b) Plant capacity and parasitic load

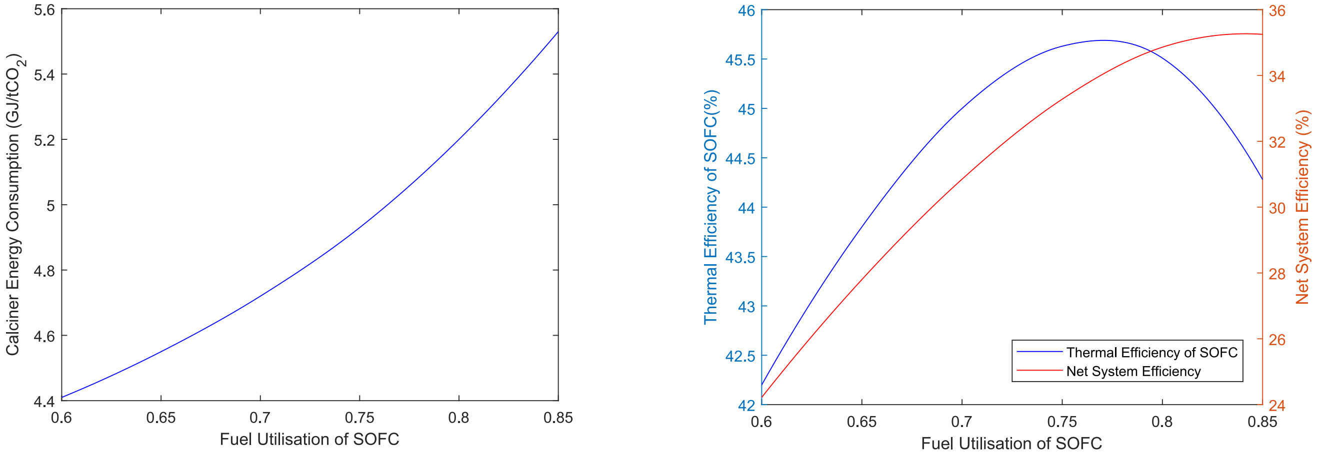

(c) Energy consumption of calciner

(d) Thermal efficiency of SOFC and net system efficiency

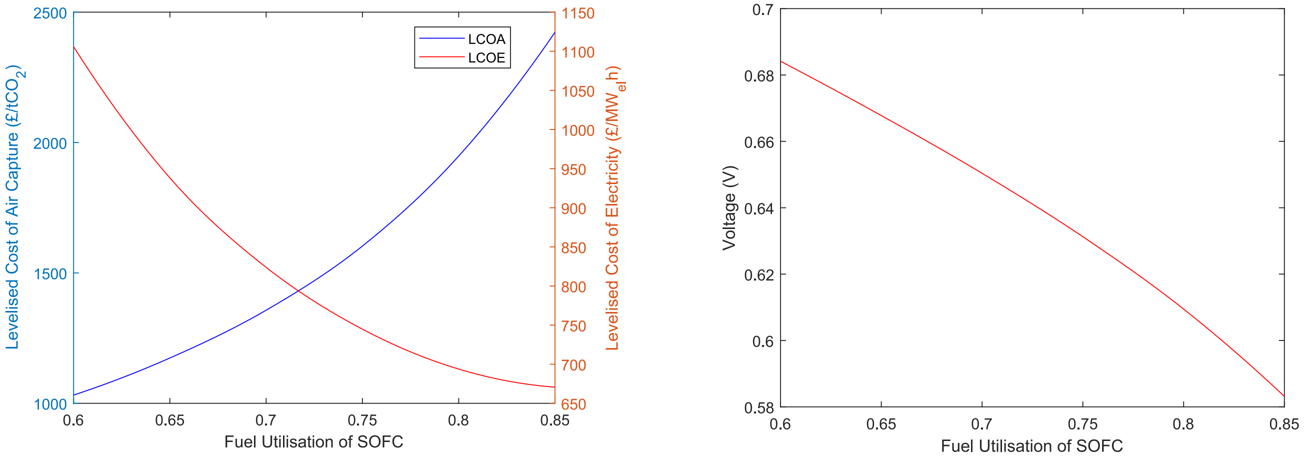

(e) LCOA and LCOE

(f) Voltage

Fig. 4. Thermodynamic and economic analyses results with different fuel utilisation efficiencies.

LCOE decreases as U_f increases, albeit at a slower rate. As *LCOE* is independent of the CO$_2$ captured, its decline is largely dependent on $\dot{W}_p$ reducing and the $\dot{W}_{net}$ increasing. However, as the η_{net} levels off with U_f in Fig. 4d, so does the rate of decrease of *LCOE* with fuel utilisation, as fuel consumption and costs increase to counteract the lessened η_{SOFC}. It remains apparent however that the *LCOA* is more sensitive to the U_f increase. Therefore, from an economic perspective, U_f should remain minimised while not compromising the SOFC's performance.

Fig. 4f shows variation of voltage with changing U_f. A significant decrease in voltage is shown when increasing U_f. Higher U_f increases the amount of hydrogen reacted at anode, meanwhile increasing the percentage of oxygen combined with electrons at cathode. Consequently, the voltage changes due to fuel composition ΔV_{anode} and due to oxidant composition ΔV_{anode} would both decrease, which directly influence the output voltage of the SOFC. As partial pressures of hydrogen and oxygen in the output steams from anode and cathode become lower, the actual output voltage of the SOFC is reduced.

Both DAC and SOFCs are commercially immature technologies, with limited certainty on prices both at present and in the future. In the proposed model, it is assumed that the cost of CE's [6] form of L-DAC will remain constant, due to the capital-intensive nature of the project and its highly specialised technology, limiting significant economies of scale in the near future. However, the price of hydrogen and the capital cost of SOFCs have more potential to change in the near future.

Hydrogen prices are given between a range of £1–15/kg, which is realistic given the volatility of electricity prices and thus the resulting cost of producing hydrogen [51]. The $CapEx_{SOFC}$ is estimated using a range of £622–12,450/kW, where kW indicates the rated DC (direct current) generation capacity, scaled linearly for simplicity [54]. The *LCOE* and *LCOA* are sensitive to both an increased $CapEx_{SOFC}$ and the price of hydrogen for fuel use in Fig. 5, however it is clear that hydrogen prices have a greater influence on both parameters, given its domination of the *OpEx* of the system.

The fundamental business model of the proposed process will be to sell the captured carbon, either to be sequestered and offset an organisation's emissions or to be transported and used for industrial processes. Therefore, to be economically viable, the price at which carbon is sold must be below the carbon tax rate, for this to be an attractive option for businesses. The minimum value of *LCOA* across all scenarios drops to £314/tCO$_2$, when hydrogen is at a price of just under £1/kg in Fig. 5a, which is anticipated to be the minimum price at which hydrogen produced through electrolysis using renewable energy will ever be economically feasible [51]. Given that anticipated carbon taxes around the world are predicted to rise to a maximum of £125/tCO$_2$ in 2030 [57], the proposed system is unlikely to be profitable, until reductions in cost can be made across the overall *CapEx* on the DAC system and SOFC stack.

4.3. 2050 Scenario

A future scenario has been created for 2050 using scaled *CapEx* and *OpEx* estimates for L-DAC from Keith et al.'s work [6], with cost estimates detailed in Table 8. The DAC plant in 2050 from Keith et al. [6] was assumed as the Nth built DAC plant, which has improved its constructability and supply chain relationships, leading reductions of 5 % in contingency cost, 5 % in engineering cost, and 20 % on material costs. In 2050 scenario, the estimate of $CapEx_{SOFC}$ considered the U.S. Department of Energy's capital cost target anticipation for SOFC stacks, which is \$207/kW$_{dc}$ of SOFC power generation capacity [54]. This is a simplified scenario in which changes in interest rates, inflation rates and exchange rates are not accounted for.

Fig. 6 displays the cost distribution for a 2050 scenario. The $CapEx_{SOFC}$ is estimated to reduce more significantly than the $CapEx_{DAC}$, given the anticipated acceleration in the adoption of the SOFC technology [50,54]. Fuel costs in Fig. 6b still are the largest single factor in the system's *OpEx*, but no longer dwarf the other elements, as they did in Fig. 3b. This significant reduction in *OpEx* as well as reduced *CapEx*, leads to an *LCOA* for this 2050 scenario of £191/tCO$_2$, which fits within the range of *LCOA* estimates in Table 8 for the CE's model [6]. While still at the higher end of these estimates, this is an economically feasible figure for two reasons: carbon taxes could foreseeably increase to this price if estimates for 2030 are £125/tCO$_2$ [57], and it is very much a possibility that in the UK and beyond, the use of natural gas will either be banned or have financial penalties in place that render it an economically unviable option for fuelling a process where alternatives are available.

Table 8
2050 cost estimations.

Parameter	Current Value	2050 Value	Reference (for 2050)
$CapEx_{DAC}$(£/tCO$_2$)	885	610	[6]
$OpEx_{DAC}$(£/tCO$_2$)	34	27	[6]
$CapEx_{SOFC}$*(£m)	45.5	11.4	[54]
$OpEx_{SOFC}$*(£m)	1.20	0.26	[54]
Price of hydrogen fuel (£/kg)	7.83	1.00	[51]

* Quoted in total price for comparison as a linear scaling method has been used for 2050 scenario.

Table 9 and Table 10 compares LCOA between the proposed system and other forms of DAC technologies, and the LCOE between the proposed system and SOFC integrated with CC system, respectively. The results show that both levelised cost of direct air capture and electricity vary widely with different technologies. Comparable LCOA of the proposed system in 2050 to other DAC technologies indicates future feasibility of integrating SOFC and renewable hydrogen into DAC. Table 9 also compares electricity and heat demands for capturing 1 tonne of CO$_2$. Proposed system in this study shows higher electricity than other DAC technologies, except for the membrane DAC. This could be due to the entire DAC process which is from the air contactor to CO$_2$ compressor having a higher parasitic load. In Table 10, the proposed system could still have a high LCOE in 2050 compared to others, suggesting that SOFC from such an integrated system may not be suitable for producing excess electricity for sale and therefore should be designed to match the size of DAC for sufficient electricity supply.

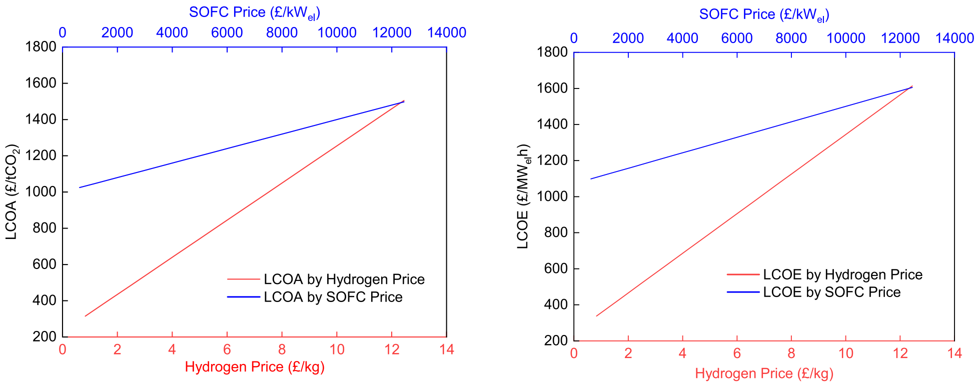

(a) Levelised cost of capture from air (LCOA)

(b) Levelised cost of electricity (LCOE)

Fig. 5. Levelised cost variation with hydrogen price and SOFC price.

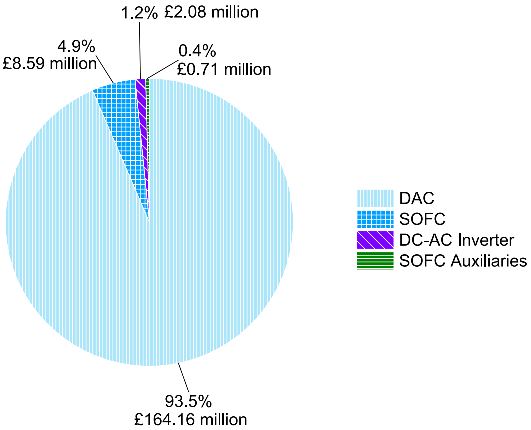

(a) Estimated 2050 CapEx distribution

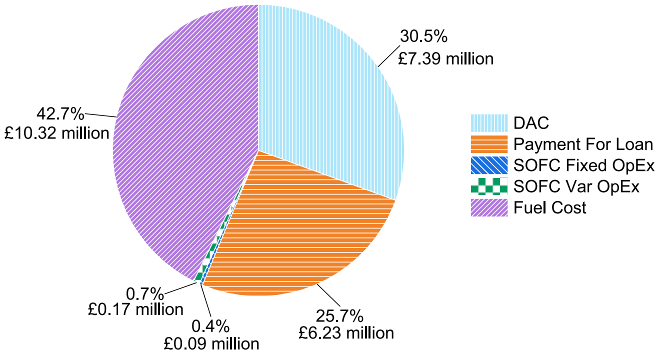

(b) Estimated 2050 OpEx distribution

Fig. 6. Estimated cost distribution under 2050 scenario.

Table 9
Comparison of different DAC technologies based on LCOA and energy requirements.

Technology	LCOA (£/tCO$_2$)	Electricity demand (kWh/tCO$_2$)	Heat demand (GJ/tCO$_2$)	Reference
Proposed system	1,013	563	4.4	–
Proposed system in 2050	191	–	–	–
Natural gas-SOFC-L-DAC	149	–	–	[8]
High temperature DAC	123–304	366	5.3	[6]
Low temperature DAC	415–498	–	–	[58]
Passive DAC using solid sorbent	116–282	400	5.76	[59]
Membrane DAC	830–8,300	3000	–	[22,60]
Aqueous amine DAC	83–830	0.403	10.7	[61]

4.4. Further work and challenges

The key technical limitations of the thermodynamic model largely surround the untested nature of the setup beyond thermodynamic simulations. Although the L-DAC model and the SOFC model individually are both proven in reality, the model integrating the two of them is currently an approximation, envisioning a theoretical heat jacket surrounding the calciner and the anode exhaust gas of the SOFC fed directly to the calciner, which presents a challenge to system stability. Further work of testing a lab-scale model and determining the inefficiencies of heat transfer to the calciner from the SOFC would benefit the proposed system. Similarly, the costs of integrating the two systems and any custom equipment should be considered in the future work to improve the economic model. As there is such large variation in the price of capital costs for key components, there seems limited value in making these more detailed estimates currently.

Table 10
Comparison of LCOE across different SOFC-CC technologies.

Technology	LCOE (£/MW$_{el}$h)	Reference
Proposed system	1,127	–
Proposed system in 2050	204	–
Natural gas-SOFC-DAC	50	[8]
Biogas-SOFC-gas turbine-CC	123	[62]
Coal-SOFC-gas turbine-CC	53–73	[63]
Natural gas-SOFC-gas turbine-CC	50–54	[63]

The current high capital costs of a SOFC and hydrogen fuel present another challenge to generate electricity at a competitive price. One possible consideration for this is to use the excess electricity generated for hydrogen electrolysis, which could partially meet the demand for fuel costs, thus reducing some operating expense. Alternative sustainable scenario could be explored by removing the SOFC altogether and studying the feasibility of simply feeding pure hydrogen as a fuel to the calciner and using renewably generated electricity to meet the parasitic load requirements of the L-DAC process. This would remove the operating and capital expenditure of the SOFC and eliminate the additional fuel costs spent on generating excess expensive electricity. Using hydrogen solely as a fuel combusted in the calciner and buying alternative renewable electricity to power the process could be a cheaper option, however its techno-economic feasibility would have to be explored, as hydrogen would no longer be delivered to the calciner in a steam mixture at 950 °C, alongside the additional indirect heat transfer from the calciner heat jacket, so an increased level of hydrogen fuel may be required to reach the required temperatures for calcination, which could compromise the potential commercial viability of such a system.

Although the L-DAC does not require farmland and can occupy relatively little space and allow for more flexible sites compared to the land use of bioenergy with carbon capture and storage technology, land use is still an important subsequent factor that determines the deployment and installation of DAC technology. Table 11 lists data on the total land areas required for L-DAC system combined with different renewable energy sources [64]. It is significant that the renewable energy sources would largely increase the total land use of L-DAC. Additional environmental impacts associated with this aspect should be involved for a comprehensive assessment. Other suggestions on the land choices indicate that L-DAC could be situated on marginal land or near the location of CO$_2$ sequestration to save the cost for CO$_2$ pipelines.

Table 11 provides useful information on the size of possible renewable energy used for L-DAC, but it lacks details on the scale of renewable energy-based electrolyser needed for hydrogen production. In this study, a capacity factor of 80 % is assumed to run the SOFC, accordingly,

Table 11
Land areas of L-DAC combined with different energy sources [64].

Combinations (based on 1Mt CO$_2$/year capture capacity)	DAC plant area (km^2)	Energy source area (km^2)
L-DAC powered by natural gas with carbon capture and storage	0.4	0.4
L-DAC powered by natural gas with carbon capture and storage and photovoltaic	0.4	7.1
L-DAC powered by natural gas with carbon capture and storage and geothermal	0.4	1.5
L-DAC powered by natural gas with carbon capture and storage and wind	0.4	13.6

24,876 tonne of hydrogen is needed per year to achieve 80 % of the SOFC's output. This amount of hydrogen corresponds to a continuous and unremitting production of hydrogen at a rate of 237.8 Nm^3/h throughout the year, equivalent to a 100 MW electrolyser. It undoubtedly poses challenges about supplying constant renewable electricity to such electrolysers. The possible size and production rate has been reported, showing that 1.5 MW wind power plant could produce hydrogen at 11,963 kg/year while 2.0 MW solar PV plant could produce 94,432 kg hydrogen per year [65]. These figures highlight the needs to accelerate scaling up the electrolyser using renewable electricity.

To estimate the potential shortfall in supply of hydrogen to SOFC, an assumption about the capacity factor ranging from 20 % to 80 % is made, representing different availabilities to supply renewable resources. Fig. 7 illustrates the results of LCOA and LOCE under these scenarios. It shows that lower supply of renewable energy for hydrogen production, i.e., lower capacity factor, leads to increased costs, which is related to significant rises in fuel costs. Considering that only about 4 % of global hydrogen is produced currently via electrolysis [66], the development of electrolysis technology itself is urgent and critical. Meanwhile hydrogen serves as an energy carrier can facilitate expansion and stable operation of renewable electricity. Although there are multiple challenges existing in the fields of hydrogen storage, transportation, water requirement, and renewable electricity prices, etc., the momentum towards hydrogen production using renewable energy is irresistible.

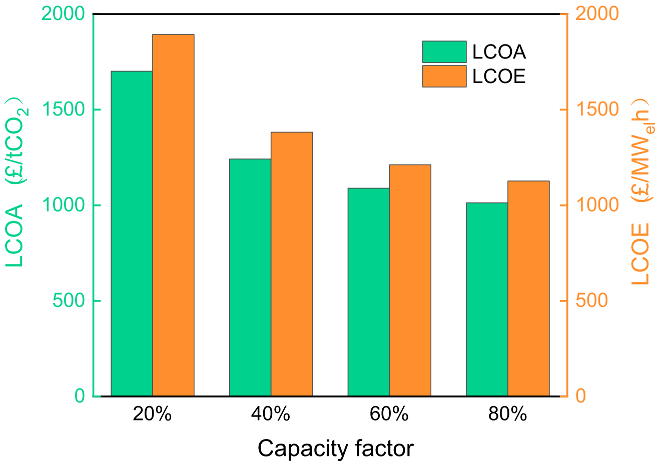

Fig. 7. Variations of LCOA and LCOE under different capacity factors.

5. Conclusion

This study aims to establish the technical and economic feasibility of a hydrogen fed solid oxide fuel cells (SOFCs) integrated with a liquid direct air capture (L-DAC) system, whereby the hydrogen is produced through electrolysis using renewable energy sources. Implications observed in the study are summarised: (1) while the model demonstrates the technical feasibility of the system, the levelised cost of capture in particular renders the proposed system using current pricing commercially infeasible; (2) when considering the current prices of carbon and electricity in the UK sit at approximately £44/tCO_2 and £120/MWh_{el} respectively, the levelised costs of both carbon capture and electricity are far too high to be economically viable or attractive to company as a carbon offsetting option; (3) the sensitivity analysis revealed that the price of hydrogen is the most influential factor in the unusually high levelised costs, aside from the unavoidable DAC capital expenditure; however, even when minimising hydrogen prices to the lowest feasible price of £1/kg using the current economic model, the levelised cost of capture of £314/tCO_2 remains too high to be economically competitive, considering that alternative natural gas fed L-DAC options can reach levelised costs of capture comfortably below £130/tCO_2; and (4) a possible 2050 cost scenario predicts a levelised cost of capture of £191/tCO_2, which is comparable with commercial estimates for natural gas fed L-DAC (£123–304/tCO_2). This study presents limitations as the proposed system is essentially 'future-proof' by adjusting the economic models, equipment and fuel of natural gas fuelled DAC systems. It is concluded that with anticipated future cost reductions for hydrogen, L-DAC and SOFCs, it is feasible that in 25 years, the system proposed could provide an economically competitive form of DAC. The future work based on the proposed model could concentrate on the testing of a lab-scale model and determining the inefficiencies of heat transfer to the calciner from the SOFCs. A comprehensive assessment of renewable-powered hydrogen production is also needed to address the challenges in hydrogen storage and transportation, renewable electricity supply and prices, etc.

CRediT authorship contribution statement

Imogen Griffiths: Writing – original draft, Software, Methodology, Investigation, Data curation, Conceptualization. **Ruiqi Wang:** Writing – review & editing, Software, Methodology, Investigation, Formal analysis. **Janie Ling-Chin:** Writing – review & editing, Visualization, Supervision, Methodology, Conceptualization. **Anthony Paul Roskilly:** Supervision, Project administration, Funding acquisition, Conceptualization.

Declaration of competing interest

The authors declare that they have no known competing financial interests or personal relationships that could have appeared to influence the work reported in this paper.

Data availability

Data will be made available on request.

Acknowledgment

This research was delivered for "A Network for Heating and Cooling Research to Enable a Net-Zero Carbon Future (H + C Zero Network)" with financial support from the UK Research Council (EP/T022906/1) and "ELEXIA" with funding in the European Commission's Horizon Europe I&A Research Programme under Grant Agreement Number 101075656.

Appendix A. Supplementary data

Supplementary data to this article can be found online at https://doi.org/10.1016/j.enconman.2024.118739.

References

[1] Singh U, Colosi LM. Capture or curtail: the potential and performance of direct air capture powered through excess renewable electricity. Energy Conversion and Management: X 2022;15:100230.
[2] Brethomé FM, Williams NJ, Seipp CA, Kidder MK, Custelcean R. Direct air capture of CO2 via aqueous-phase absorption and crystalline-phase release using concentrated solar power. Nat Energy 2018;3:553–9.
[3] International Energy Agency, Direct Air Capture 2022, IEA, Paris https://www.iea.org/reports/direct-air-capture-2022 (accessed July 28, 2023).
[4] Bouaboula H, Chaouki J, Belmabkhout Y, Zaabout A. Comparative review of Direct air capture technologies: from technical, commercial, economic, and environmental aspects. Chem Eng J 2024;484:149411.
[5] Jiang L, Liu W, Wang RQ, Gonzalez-Diaz A, Rojas-Michaga MF, Michailos S, et al. Sorption direct air capture with CO2 utilization. Prog Energy Combust Sci 2023;95:101069.
[6] Keith DW, Holmes G, St D, Angelo KH. A process for capturing CO2 from the atmosphere. Joule 2018;2:1573–94.
[7] K. Lackner, H.-J. Ziock, P. Grimes. Carbon Dioxide Extraction from Air: Is It An Option? . US Department of Energy (United States). 1999. https://www.osti.gov/biblio/770509 (accessed July 28, 2023).

[8] Hanak DP, Jenkins BG, Kruger T, Manovic V. High-efficiency negative-carbon emission power generation from integrated solid-oxide fuel cell and calciner. Appl Energy 2017;205:1189–201.

[9] Holmes G, Keith DW. An air-liquid contactor for large-scale capture of CO2 from air. Philos Trans R Soc A Math Phys Eng Sci 2012;370:4380–403.

[10] E. National Academies of Sciences, Medicine, E. Division on, S. Life, B. Ocean Studies, S. Board on Chemical, et al. Negative Emissions Technologies and Reliable Sequestration: A Research Agenda. Chapter 5: Direct Air Capture. National Academies Press (US) Copyright 2019 by the National Academy of Sciences. All rights reserved., Washington (DC), 2018.

[11] Terlouw T, Treyer K, Bauer C, Mazzotti M. Life cycle assessment of direct air carbon capture and storage with low-carbon energy sources. Environ Sci Tech 2021;55:11397–411.

[12] Breyer C, Fasihi M, Aghahosseini A. Carbon dioxide direct air capture for effective climate change mitigation based on renewable electricity: a new type of energy system sector coupling. Mitig Adapt Strat Glob Chang 2020;25:43–65.

[13] Wohland J, Witthaut D, Schleussner C-F. Negative emission potential of direct air capture powered by renewable excess electricity in Europe. Earth’s Future 2018;6:1380–4.

[14] Madhu K, Pauliuk S, Dhathri S, Creutzig F. Understanding environmental trade-offs and resource demand of direct air capture technologies through comparative life-cycle assessment. Nat Energy 2021;6:1035–44.

[15] Ferrario D, Stendardo S, Verda V, Lanzini A. Solar-driven calcium looping system for carbon capture in cement plants: process modelling and energy analysis. J Clean Prod 2023;394:136367.

[16] Li C, Shi H, Cao Y, Kuang Y, Zhang Y, Gao D, et al. Modeling and optimal operation of carbon capture from the air driven by intermittent and volatile wind power. Energy 2015;87:201–11.

[17] Prats-Salvado E, Jagtap N, Monnerie N, Sattler C. Solar-powered direct air capture: techno-economic and environmental assessment. Environ Sci Tech 2024;58:2282–92.

[18] Ishaq H, Crawford C. Potential of offshore wind energy for direct air capture. Int J Energy Res 2022;46:18919–27.

[19] Breyer C, Fasihi M, Bajamundi C, Creutzig F. Direct air capture of CO2: a key technology for ambitious climate change mitigation. Joule 2019;3:2053–7.

[20] McQueen N, Psarras P, Pilorgé H, Liguori S, He J, Yuan M, et al. Cost analysis of direct air capture and sequestration coupled to low-carbon thermal energy in the United States. Environ Sci Tech 2020;54:7542–51.

[21] Albert MDA, Bennett KO, Adams CA, Gluyas JG. Waste heat mapping: a UK study. Renew Sustain Energy Rev 2022;160:112230.

[22] Erans M, Sanz-Pérez ES, Hanak DP, Clulow Z, Reiner DM, Mutch GA. Direct air capture: process technology, techno-economic and socio-political challenges. Energ Environ Sci 2022;15:1360–405.

[23] Weber A. Fuel flexibility of solid oxide fuel cells. Fuel Cells 2021;21:440–52.

[24] Abdelkareem MA, Lootah MA, Sayed ET, Wilberforce T, Alawadhi H, Yousef BAA, et al. Fuel cells for carbon capture applications. Sci Total Environ 2021;769:144243.

[25] Rao M, Fernandes A, Pronk P, Aravind PV. Design, modelling and techno-economic analysis of a solid oxide fuel cell-gas turbine system with CO2 capture fueled by gases from steel industry. Appl Therm Eng 2019;148:1258–70.

[26] Zhang Y, Wu S, Cui D, Yoon S-J, Bae Y-S, Park B, et al. Energy and CO2 emission analysis of a Bio-Energy with CCS system: biomass gasification-solid oxide fuel cell-mini gas turbine-CO2 capture. Fuel Process Technol 2022;238:107476.

[27] Santarelli M, Briesemeister L, Gandiglio M, Herrmann S, Kuczynski P, Kupecki J, et al. Carbon recovery and re-utilization (CRR) from the exhaust of a solid oxide fuel cell (SOFC): analysis through a proof-of-concept. J CO2 Util 2017;18:206–21.

[28] Nabavi SA, Erans M, Manović V. Demonstration of a kW-scale solid oxide fuel cell-calciner for power generation and production of calcined materials. Appl Energy 2019;255:113731.

[29] Erans M, Nabavi SA, Manović V. Pilot-scale calcination of limestone in steam-rich gas for direct air capture. Energy Conversion and Management: X 2019;1:100007.

[30] Hanak DP, Manovic V. Combined heat and power generation with lime production for direct air capture. Energ Conver Manage 2018;160:455–66.

[31] Daniel T, Masini A, Milne C, Nourshagh N, Iranpour C, Xuan J. Techno-economic analysis of direct air carbon capture with CO2 utilisation. Carbon Capture Sci & Technol 2022;2:100025.

[32] An K, Farooqui A, McCoy ST. The impact of climate on solvent-based direct air capture systems. Appl Energy 2022;325:119895.

[33] Moreno-Gonzalez M, Berger A, Borsboom-Hanson T, Mérida W. Carbon-neutral fuels and chemicals: economic analysis of renewable syngas pathways via CO2 electrolysis. Energ Conver Manage 2021;244:114452.

[34] Prats-Salvado E, Monnerie N, Sattler C. Techno-economic assessment of the integration of direct air capture and the production of solar fuels. Energies 2022;15:5017.

[35] Coppitters D, Costa A, Chauvy R, Dubois L, De Paepe W, Thomas D, et al. Energy, exergy, economic and environmental (4E) analysis of integrated direct air capture and CO2 methanation under uncertainty. Fuel 2023;344:127969.

[36] Datta A, Krishnamoorti R. Analysis of direct air capture integrated with wind energy and enhanced oil recovery. Environ Sci Tech 2023;57:2084–92.

[37] Sabatino F, Gazzani M, Gallucci F, van Sint Annaland M. Modeling, optimization, and techno-economic analysis of bipolar membrane electrodialysis for direct air capture processes. Ind Eng Chem Res 2022;61:12668–79.

[38] Sagues WJ, Park S, Jameel H, Sanchez DL. Enhanced carbon dioxide removal from coupled direct air capture–bioenergy systems. Sustainable Energy Fuels 2019;3:3135–46.

[39] Zhang W, Croiset E, Douglas PL, Fowler MW, Entchev E. Simulation of a tubular solid oxide fuel cell stack using AspenPlusTM unit operation models. Energ Conver Manage 2005;46:181–96.

[40] S. Bianchi. Process modelling of a Direct Air Capture (DAC) system based on the Kraft process. 2018. https://webthesis.biblio.polito.it/9262/1/tesi.pdf (accessed July 28, 2023).

[41] Hussain S, Yangping L. Review of solid oxide fuel cell materials: cathode, anode, and electrolyte. Energy Transitions 2020;4:113–26.

[42] Malzbender J, Wessel E, Steinbrech RW. Reduction and re-oxidation of anodes for solid oxide fuel cells. Solid State Ion 2005;176:2201–3.

[43] Samanta S, Roy D, Roy S, Smallbone A, Paul Roskilly A. Modelling of hydrogen blending into the UK natural gas network driven by a solid oxide fuel cell for electricity and district heating system. Fuel 2024;355:129411.

[44] Duan L, Huang K, Zhang X, Yang Y. Comparison study on different SOFC hybrid systems with zero-CO2 emission. Energy 2013;58:66–77.

[45] Ni M, Leung DYC, Leung MKH. Thermodynamic analysis of ammonia fed solid oxide fuel cells: comparison between proton-conducting electrolyte and oxygen ion-conducting electrolyte. J Power Sources 2008;183:682–6.

[46] Zheng N, Zhang H, Duan L, Wang Q, Bischi A, Desideri U. Techno-economic analysis of a novel solar-driven PEMEC-SOFC-based multi-generation system coupled parabolic trough photovoltaic thermal collector and thermal energy storage. Appl Energy 2023;331:120400.

[47] Fuel Cell Handbook (Seventh Edition). U.S. Department of Energy. Office of Fossil Energy. National Energy Technology Laboratory2004.

[48] Campanari S. Thermodynamic model and parametric analysis of a tubular SOFC module. J Power Sources 2001;92:26–34.

[49] Jiang P, Mahmud Parvez A, Meng Y, Dong X, Xu M, Luo X, et al. Novel two-stage fluidized bed-plasma gasification integrated with SOFC and chemical looping combustion for the high efficiency power generation from MSW: a thermodynamic investigation. Energ Conver Manage 2021;236:114066.

[50] Elcogen to build 50 MW SOFC manufacturing facility at Ülemiste City campus in Estonia. Fuel Cells Bulletin. 2021;3:1-1. https://doi.org/10.1016/S1464-2859(21)00115-2.

[51] Green Hydrogen: Optimising Net Zero. Renewable UK. 2022. https://www.renewableuk.com/news/604418/Green-Hydrogen-Optimising-Net-Zero.htm (accessed July 28, 2023).

[52] J.S.J. Hamilton. Renewable PPAs and a review of the commodity price spike on renewable hydrogen production costs. Independent Commodity Intelligence Services. 2022. https://www.icis.com/explore/resources/news/2022/10/11/10813598/icis-whitepaper-renewable-ppas-and-a-review-of-the-commodity-price-spike-on-renewable-hydrogen-production-costs/ (accessed July 28, 2023).

[53] Campanari S, Chiesa P, Manzolini G, Bedogni S. Economic analysis of CO2 capture from natural gas combined cycles using molten carbonate fuel cells. Appl Energy 2014;130:562–73.

[54] Whiston MM, Azevedo IML, Litster S, Samaras C, Whitefoot KS, Whitacre JF. Meeting U.S. Solid Oxide Fuel Cell Targets. Joule 2019;3:2060–5.

[55] ExchangeRates.org.uk, ’US Dollar to British Pound Spot Exchange Rates for 2023’, Mar. 2023. https://www.exchangerates.org.uk/USD-GBP-spot-exchange-rates-history-2023.html (accessed Mar. 28, 2023).

[56] Trading Economics, UK Electricity Spot Prices. 2023. https://tradingeconomics.com/united-kingdom/electricity-price (accessed July 28, 2023).

[57] State and Trends of Carbon Pricing. The World Bank. 2022. http://hdl.handle.net/10986/37455 (accessed July 28, 2023).

[58] Abanades JC, Criado YA, Fernández JR. An air CO2 capture system based on the passive carbonation of large Ca(OH)2 structures. Sustainable Energy Fuels 2020;4:3409–17.

[59] McQueen N, Gomes KV, McCormick C, Blumanthal K, Pisciotta M, Wilcox J. A review of direct air capture (DAC): scaling up commercial technologies and innovating for the future. Progress in Energy 2021;3:032001.

[60] Castel C, Bounaceur R, Favre E. Membrane processes for direct carbon dioxide capture from air: possibilities and limitations. Frontiers in Chemical Eng 2021;3.

[61] Kiani A, Jiang K, Feron P. Techno-economic assessment for CO2 capture from air using a conventional liquid-based absorption process. Front Energy Res 2020;8.

[62] Owebor K, Diemuodeke EO, Briggs TA. Thermo-economic and environmental analysis of integrated power plant with carbon capture and storage technology. Energy 2022;240:122748.

[63] Slater JD, Chronopoulos T, Panesar RS, Fitzgerald FD, Garcia M. Review and techno-economic assessment of fuel cell technologies with CO2 capture. Int J Greenhouse Gas Control 2019;91:102818.

[64] H.L.-B. Katie Lebling, Zach Byrum, Liz Bridgwater. (2022) 6 Things to Know About Direct Air Capture. https://www.wri.org/insights/direct-air-capture-resource-considerations-and-costs-carbon-removal (accessed May 08,2024).

[65] Hassan Q, Sameen AZ, Salman HM, Jaszczur M. Large-scale green hydrogen production via alkaline water electrolysis using solar and wind energy. Int J Hydrogen Energy 2023;48:34299–315.

[66] IRENA (2018), Hydrogen from renewable power: Technology outlook for the energy transition, International Renewable Energy Agency, Abu Dhabi. https://www.irena.org/publications/2018/Sep/Hydrogen-from-renewable-power (accessed on May 09, 2024).